

*Journal of Organometallic Chemistry*, 370 (1989) 357–381  
Elsevier Sequoia S.A., Lausanne – Printed in The Netherlands  
JOM 09810

**Transition metal catalyzed asymmetric cross coupling reactions.  
New ligands and the effects of added salts. Crystal structures  
of  $[\text{Ph}_2\text{PCH}_2\text{CH}\{(\text{CH}_2)_3\text{SMe}\}\text{NMe}_2] \cdot \text{PdCl}_2$   
and  $[\text{Ph}_2\text{PCH}_2\text{CH}\{(\text{CH}_2)_2\text{SMe}\}\text{NMe}_2] \cdot \text{PdCl}_2$**

**Graham Cross \***, **Bindert K. Vriesema \*\***, **Gerd Boven**, **Richard M. Kellogg \***,

*Department of Organic Chemistry, University of Groningen, Nijenborgh 16,  
9747 AG Groningen (The Netherlands)*

and **F. van Bolhuis**,

*Department of Chemistry, X-Ray Service, University of Groningen, Nijenborgh 16,  
9747 AG Groningen (The Netherlands)*

(Received November 3rd, 1988)

**Abstract**

Tridentate ligands have been derived from the amino acids lysine, methionine, methionine sulfoxide, and homomethionine by dimethylation at nitrogen and reduction of the carboxyl group followed by substitution of hydroxyl by the diphenylphosphino group. These ligands are effective in promoting the  $\text{Ni}^0$  or  $\text{Pd}^0$  catalyzed cross coupling of the Grignard reagent of 1-chloro-1-phenylethane with vinyl bromide. The enantiomeric excesses found for coupling product formed in the presence of these ligands exceed those expected on the grounds solely of a steric effect of the amino acid side chain. A special effect of the heteroatom in the side chain is indicated. X-ray diffraction studies of the  $\text{PdCl}_2$  complexes of the ligands derived from methionine and homomethionine confirm the expected coordination of the transition metal atom by the phosphino and amino centers and reveal that there is no significant ligation of sulfide in these dipositive cations.

Not only heteroatoms in the side chain but also the presence of other metal cations in solution profoundly affect the course of reaction. When  $\text{ZnBr}_2$  is added to the Grignard reagent derived from 1-chloro-1-phenylethane, the rate of  $\text{Ni}^0$  or  $\text{Pd}^0$  catalyzed coupling with vinyl bromide increases and the direction of the enantioselection is reversed. Similar effects are observed with  $\text{ZnI}_2$ , but  $\text{ZnCl}_2$  has a pronounced inhibitory effect on the cross coupling. Other added salts have little

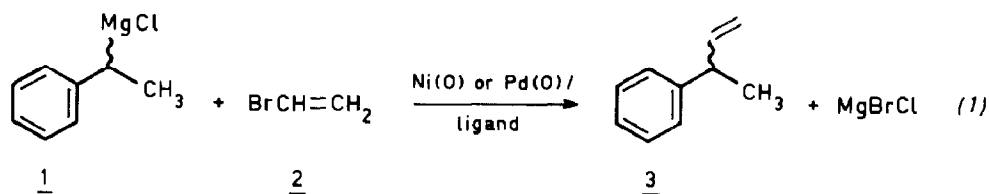
\* Present address: Unilever Research Laboratories, Vlaardingen, The Netherlands.

\*\* Present address: Dutch State Mines (DSM), Geleen, The Netherlands.

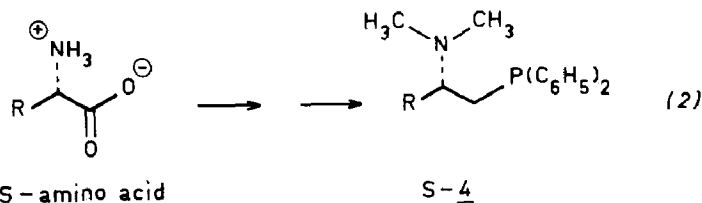
effect. This switch in enantioselectivity induced by zinc halides allows a formal synthesis of the analgesic ibuprofen starting from use of a single chiral ligand in the Ni<sup>0</sup> catalyzed cross coupling of (4-isobutyl)-1-phenyl-1-chloroethane with vinyl bromide. Subsequent oxidation of the double bond leads to ibuprofen, the enantiomer obtained depending on the reaction conditions.

## Introduction

We studied the design and synthesis of chiral macrocyclic compounds that could act as frameworks on which nickel- or palladium-catalyzed bond forming reactions could occur [1]. This led us to some ideas on stereoelectronic factors that could be tested with structurally less complex ligands [2\*]. The reaction initially studied is represented in eq. 1. With the aid of chiral ligands the cross coupling adduct, 3-phenyl-1-butene (**3**) can be obtained in enantiomerically enriched form. This was



shown originally by Consiglio et al. [3] and Kumada and Hayashi [4]. The latter authors also discovered that ligands **4**, derived from readily available amino acids as indicated in eq. 2, are quite effective in this cross coupling [5].



An excellent opportunity for testing various principles of ligand design is presented by compounds **4**. Systematic modification of the structurally variable portion of the molecule, in order to examine structure-reactivity relationships, allows testing of various theories. A reasonable amount of information is available for analysis of the relationship between differences in the structure of **4** and the absolute configuration of the major enantiomer of the coupling product **3** (eq. (1) [5,6,7\*]). The side chain substituent **R** always begins with a carbon atom, which can carry up to three branches. This carbon is designated as  $\alpha$  and subsequent atoms in the chain (not necessarily carbon atoms) as  $\beta$ ,  $\gamma$ , etc.

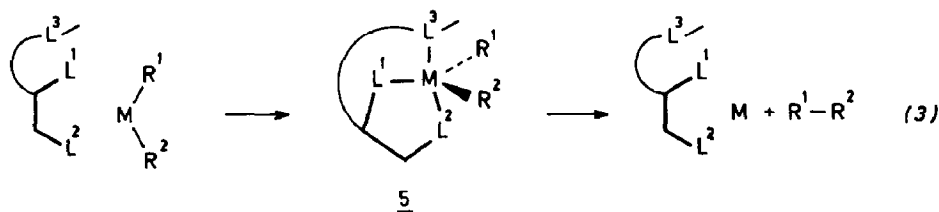
From published data [5,6] it can be seen that the ligands **4** of the *S*-configuration always give rise to coupling products **3** also of the *S*-configuration. (In some cases the *R*-ligands were synthesized because only the *R*-amino acids were synthetically available). Moreover the enantiomeric excess (e.e.) of **3** increases fairly predictably as a function of chain branching for **R** groups that consist purely of carbon chains.

\* Reference number with asterisk indicates a note in the list of references.

$R \equiv \begin{array}{c} \alpha \quad \beta \quad \gamma \quad \delta \\ -C-A-B-C \\   \end{array}$	group R	branching
<u>a</u>	CH <sub>3</sub> -	-
<u>b</u>	(CH <sub>3</sub> ) <sub>2</sub> CHCH <sub>2</sub> -	1 $\alpha$ , 2 $\beta$
<u>c</u>	C <sub>6</sub> H <sub>5</sub> CH <sub>2</sub> -	1 $\alpha$
<u>d</u>	(CH <sub>3</sub> ) <sub>2</sub> CH-	2 $\alpha$
<u>e</u>	CH <sub>3</sub> CH <sub>2</sub> CH(CH <sub>3</sub> )-	2 $\alpha$ , 1 $\beta$
<u>f</u>	(CH <sub>3</sub> ) <sub>3</sub> C-	3 $\alpha$
<u>g</u>	CH <sub>3</sub> SCH <sub>2</sub> -	1 $\alpha$ , 1 $\beta$
<u>h</u>	CH <sub>3</sub> S(CH <sub>2</sub> ) <sub>2</sub> -	1 $\alpha$ , 1 $\beta$ , 1 $\delta$
<u>i</u>	(CH <sub>3</sub> ) <sub>2</sub> C(SCH <sub>3</sub> )-	2 $\alpha$ , 1 $\beta$

(A qualitative summary is given here; the original literature [5,6] gives numerical values) [7\*]. An increase of 19–21% in e.e. is obtained per  $\alpha$ -branch. The effect of  $\beta$ -branching is smaller an increase in e.e. of 0–10% being observed. Virtually no effect on the e.e.'s results from  $\gamma$ -branching. Clearly the steric bulk of the side chain substituent influences the enantioselectivity in a straightforward manner. There are two possible anomalies in this general picture of steric effects, however. For R = CH<sub>3</sub>S(CH<sub>2</sub>)<sub>2</sub> (**4h**) the e.e. of **3** is 25–30% higher than expected, and for R = (CH<sub>3</sub>)<sub>2</sub>C(SCH<sub>3</sub>) (**4i**) about 50% lower than expected from extrapolation of the above analysis.

Can factors other than steric be used to influence the e.e.'s? This is important in any consideration of design of ligands. Two possibilities can be considered briefly. Both involve the introduction of an extra coordination site into the substituent R of the amino acid. The anomalous results just mentioned for **4h**, **4i** illustrate this. A ligating site in the side arm could conceivably participate in the reductive elimination process, as illustrated schematically in eq. 3.



For M = Ni<sup>0</sup> there is both experimental and theoretical evidence that the reductive elimination step may involve change from a square planar [8] to a pentacoordinate nickel intermediate [9] at the stage of reductive elimination, this intermediate being formed by intermolecular addition of an extra ligand [10\*,11\*]. An intramolecular variation might allow extra stereochemical control via the tricyclic intermediate **5**.

Another possibility is that lone pairs available on heteroatoms in the side chain substituent may provide a coordinating site for the organometallic reagent (Grignard reagent) to be coupled [12\*]. This could lead to higher rates; whether the

enantioselectivities would be enhanced is not readily predictable owing to the absence of a detailed stereochemical model.

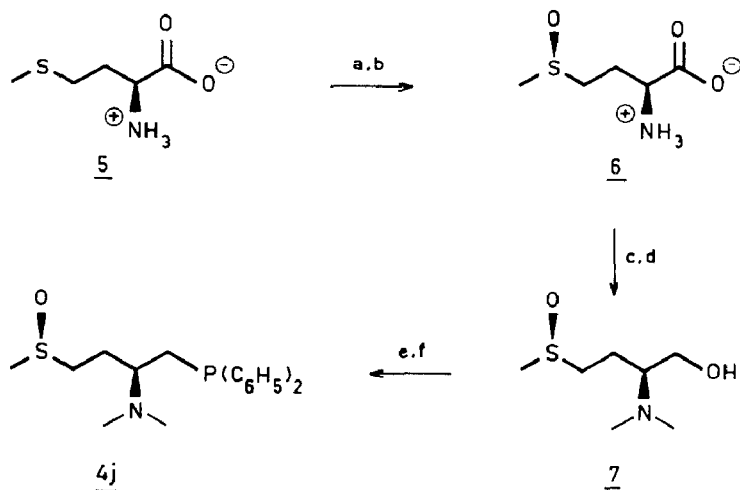
These considerations are qualitative and do not give rise to any exact model that would explain the absolute stereochemistry of **3**. Evidence will be given that the postulated coordination of the metal center in a bidentate 1,4-fashion to phosphorus and nitrogen does indeed occur. The extra ligating atoms chosen for the side chain are sulfur and nitrogen, both of which can be introduced via obtainable amino acids. It will be shown that these extra ligating atoms do participate in the coupling, and that the metal ions associated with the carbanionic species via these extra ligating sites can have a pronounced effect on the course of the reaction.

## Results

### A. Synthesis

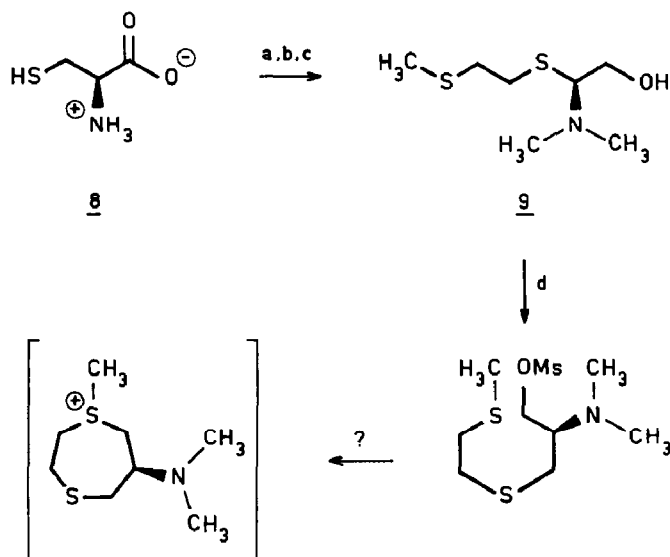
The results with **4h** ( $R = \text{CH}_3\text{SCH}_2\text{CH}_2-$ ) [6] were encouraging in that the e.e. of **3** was higher than expected purely for a steric effect. The synthesis of **4h** was modified (see Experimental) to the point that overall conversions of greater than 50% from *S*-methionine were achieved. This synthetic approach was used essentially unchanged for the preparation of other ligands. Oxidation of *S*-methionine (**5**) affords two diastereomeric methionine sulfoxides [13]; the *S*-methionine-*S*-sulfoxide diastereomer **6** can be isolated by previously described procedures [14], and is readily converted by methylation [15], esterification [16], and reduction with  $\text{LiAlH}_4$  [17], followed by substitution with diphenylphosphide, into ligand **4j** (Scheme 1).

Similarly ligand (**4k**) was obtained from *S*-lysine. More difficulty was encountered in attempts to introduce longer side arms in which sulfur is incorporated.



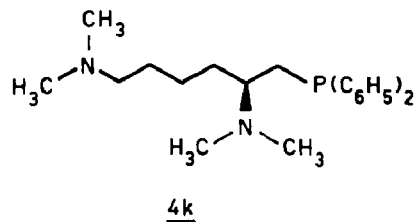
a)  $\text{H}_2\text{O}_2$ ; b) picric acid, recryst.; c)  $\text{LiAlH}_4$ ; d)  $\text{HCO}_2\text{H} \cdot \text{CH}_2\text{O}$   
 e)  $\text{CH}_3\text{SO}_2\text{Cl} / (\text{C}_2\text{H}_5)_3\text{N}$ ; f)  $(\text{C}_6\text{H}_5)_2\text{PH} \cdot \text{KOC}(\text{CH}_3)_3$

Scheme 1



a)  $\text{LiAlH}_4$ ; b)  $\text{NaOH}/\text{CH}_3\text{I}$ ; c)  $\text{HCO}_2\text{H}, \text{CH}_2\text{O}$ ; d)  $\text{CH}_3\text{SO}_2\text{Cl}, (\text{C}_2\text{H}_5)_3\text{N}$

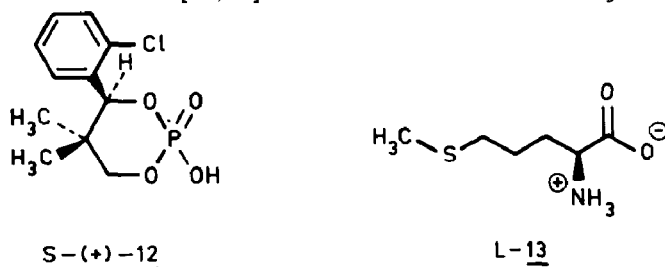
Scheme 2

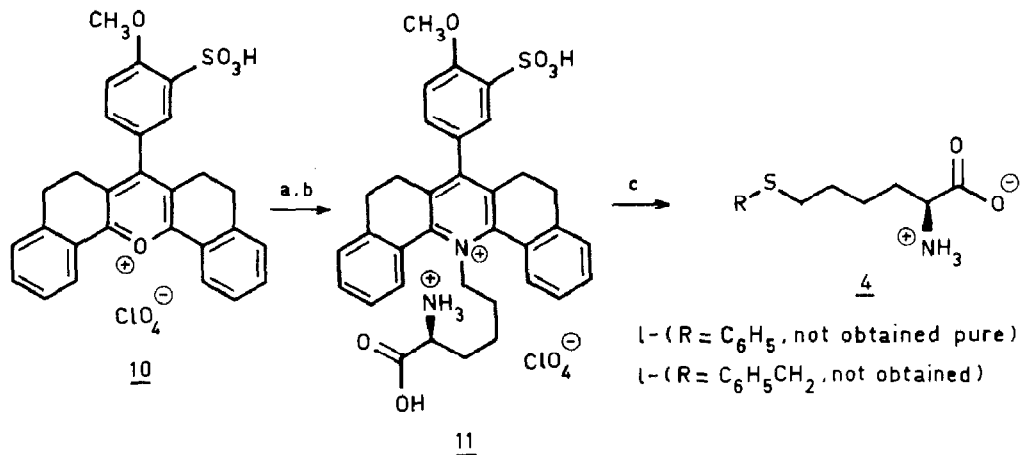


From *S*-cysteine (**8**) the chain lengthened derivative (**9**) is readily obtained. Attempts to substitute the hydroxyl group failed, probably because of cyclization as illustrated in Scheme 2.

An attempt was made to substitute the  $\delta$ -amino group of L-lysine by the procedure described by Katritzky et al. [18], in which this more basic amino group reacts selectively with pyrilium salt **10**, as shown in Scheme 3. Substitution of **11** with phenylthiol (in our hands benzylthiol was even less suitable) produced a gum, which on "trituration with ethanol" as described [18] should yield the sulfur containing amino acid. On a 3 mmol scale a little **41** ( $\text{R} = \text{C}_6\text{H}_5$ ) was obtained. An attempt to scale up to 0.5 mol was because the gum was completely intractable.

Homomethionine (**13**), which bears a trimethylene chain, is readily obtainable in racemic form [19,20]. Resolution was achieved by use of **12**, reported by Wynberg





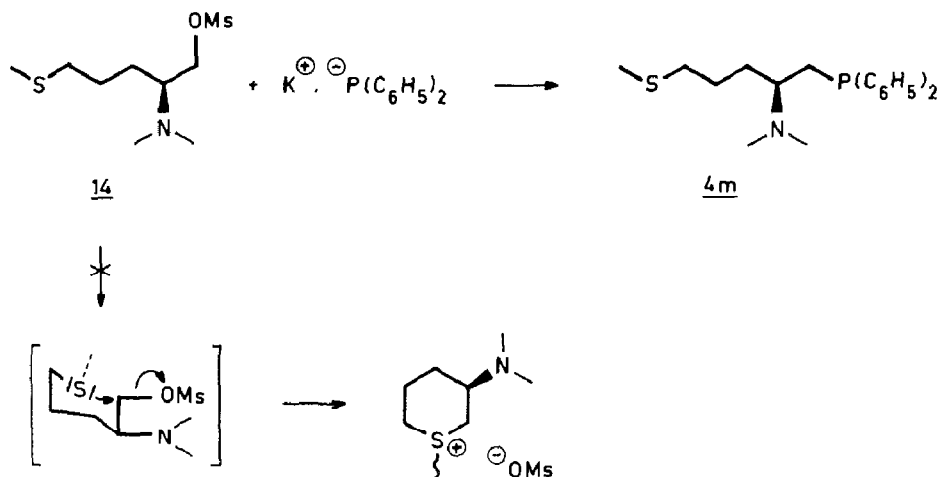
a) 10 M NaOH, L-lysine, HCl; b) 10% HClO<sub>4</sub>; c) RSH, KOH, H<sub>2</sub>O, N<sub>2</sub>

Scheme 3

and Ten Hoeve [21]. Scaling of this procedure to give quantities of **4m** needed was difficult. As described elsewhere [2], racemic **4m** can be resolved on a large scale with a crude peptidase from *Pseudomonas putida*. Enantiomerically pure *S*- and *R*-**13** are obtained in large quantities by this procedure.

The choice of **13** for conversion to **4m** was made taking account of the failure depicted in Scheme 2. At the critical stage of the mesylate **14** (Scheme 4) it was expected that intramolecular cyclization would be inhibited because in the chain conformation leading to cyclization the dimethylamino substituent would be located equatorially and would inhibit departure of mesylate in the required linear S<sub>N</sub>2 transition state [23]. In the event **4m** was obtained in 47% yield from *R*-**13**.

The enantiomeric purities (> 98%) of the ligands **4** were established at the alcohol stage prior to substitution of the mesylate (for example **14**) by diphenylphosphide anion. As described in the Experimental Section, use of europium shift



Scheme 4

reagent allowed determination of the enantiomeric excesses. We assume that no racemization occurs during the substitution by diphenyl phosphide.

### B. Crystal structures

All attempts to obtain crystalline Ni<sup>II</sup> or Ni<sup>0</sup> complexes failed. This parallels the experience of Kumada et al. [5]. These authors did obtain, however, a crystalline complex from *S*-**4d** (R = (CH<sub>3</sub>)<sub>2</sub>CH) on treatment with PdCl<sub>2</sub>·(C<sub>6</sub>H<sub>5</sub>CN)<sub>2</sub> in benzene. The crystal structure of this complex has not to our knowledge been described. With ligand **4h** under the same conditions a yellow solid complex was obtained, which was recrystallized from CH<sub>2</sub>Cl<sub>2</sub>/hexane. <sup>1</sup>H NMR data indicated complexation of the amino and phosphino groups. In CH<sub>2</sub>Cl<sub>2</sub> the singlet N(CH<sub>3</sub>)<sub>2</sub> resonance in the free ligand at δ 2.11 was shifted downfield in the complex, and appeared as two singlets, at δ 2.97 and 3.12. The singlet CH<sub>3</sub>S signal at δ 2.00 in the free ligand was not significantly shifted in the complex, which suggests that the sulfide is not ligated.

This picture was confirmed by single crystal X-ray study. A single molecule of **4h**·PdCl<sub>2</sub> is illustrated in Fig. 1 and a stereoplot is given in Fig. 2. Hydrogen positions were not determined. The expected bidentate, but not tridentate, ligation in the Pd<sup>II</sup> complex, is confirmed. The sulfur bearing side chain is twisted back somewhat. The closest sulfur–Pd<sup>II</sup> approach is 4.703 Å, which is not within ligating distance.

Ligand **4m** under the conditions described for **4h** also gave a yellow crystalline complex with PdCl<sub>2</sub>. The N(CH<sub>3</sub>)<sub>2</sub> resonances in CD<sub>2</sub>Cl<sub>2</sub> were observed at δ 2.93 and 3.10, compared with the singlet at δ 2.11 shown by the free ligand. Again, the signal from the SCH<sub>3</sub> group was barely shifted (0.05 ppm downfield) relative to that of the free ligand. A single molecule of **4m**·PdCl<sub>2</sub> is illustrated in Fig. 3 and in Fig. 4 a stereoplot is presented. The coordination is, as expected, through nitrogen and phosphorus. There is no indication of coordination to the sulfur atom. All bond lengths and bond angles are normal.

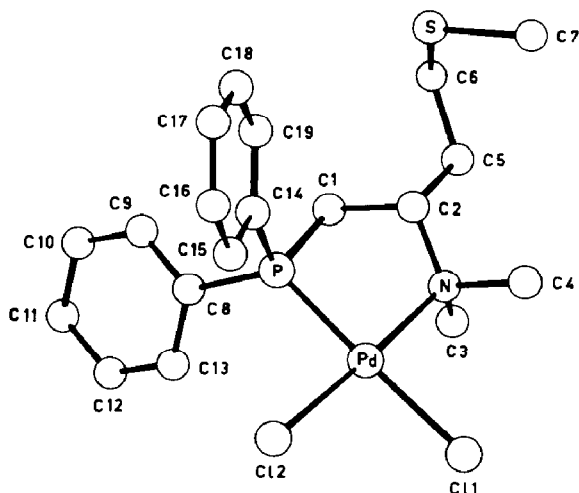


Fig. 1. Single molecule of complex **4h**·PdCl<sub>2</sub> with atom numbering scheme.

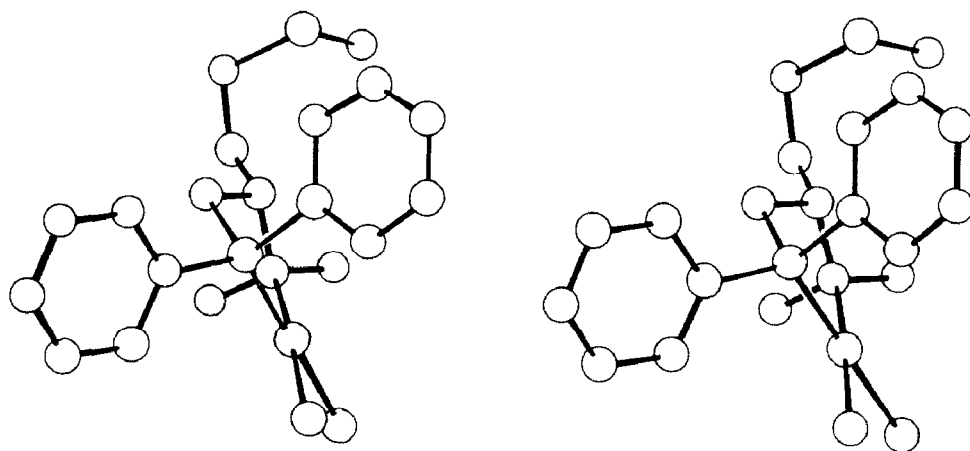


Fig. 2. Stereoplot of complex **4h**·PdCl<sub>2</sub>.

Treatment of sulfoxide **4j** with PdCl<sub>2</sub>·(C<sub>6</sub>H<sub>5</sub>CN) under conditions similar to those described gave a solid complex, but all attempts to recrystallize it failed. The ligand **4k** derived from *S*-lysine, however, gave a solid complex. No attempt was made to carry out a single crystal X-ray study, but in the <sup>1</sup>H NMR spectrum the N(CH<sub>3</sub>)<sub>2</sub> group that gives rise to a singlet at δ 2.20 for the free ligand, gave two singlets, at δ 2.99 and 3.15, indicative of coordination to Pd. The other N(CH<sub>3</sub>)<sub>2</sub> resonance, assigned to the δ-amino group, moved from δ 2.21 in the free ligand to δ 2.18 in the complex, consistent with no detectable association of this group with the Pd atom.

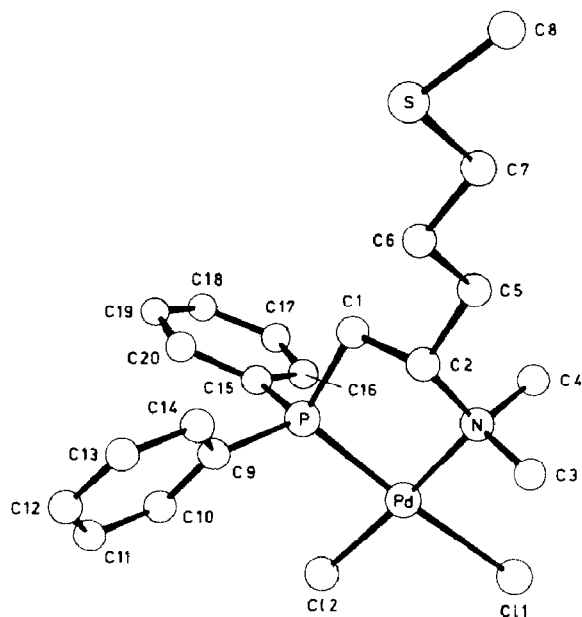


Fig. 3. Single molecule of complex **4m**·PdCl<sub>2</sub> with atom numbering scheme.



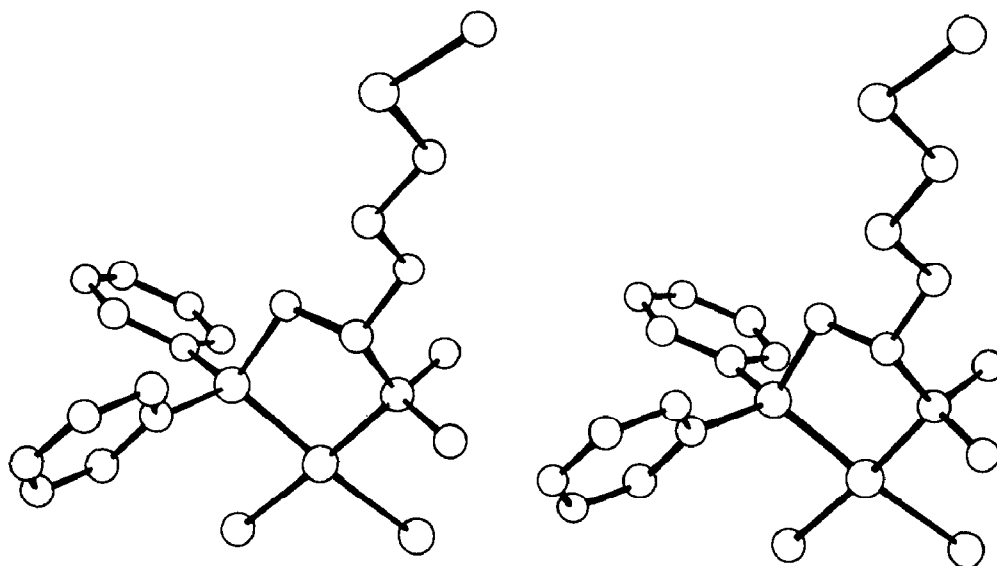


Fig. 4. Stereoplot of complex  $4m \cdot PdCl_2$ .

### C. Use of ligands in coupling reactions

The enantioselective formation of **3** (eq. 1) was used as the model reaction. The limiting reagent is vinyl bromide and the ratio of this reagent to metal-ligand complex was held at 125/1. The results for  $NiCl_2$  and  $PdCl_2$  catalyzed reactions are given in Table 1. Yields of the cross couplings were in all cases  $> 90\%$ , and are therefore not reported separately.

### D. The effect of zinc halides

In conjunction with the design of ligands **4** the effect of other parameters on the formation of **3** was examined. The catalytic efficiency in nickel is in most cases quite high, and we soon chose to run the reactions at 1000/1 ratio of vinyl bromide **2** (limiting reagent) to nickel/ligand. This allows very efficient use of the designed

Table 1

Enantiomeric excesses of **3** obtained by use of various ligands **4**<sup>a</sup>

Ligand <b>4</b>		Enantiomeric excess <b>3</b> (config.)			
Config.	R	$NiCl_2$ <sup>b,c</sup>	$NiCl_2$ <sup>b,d</sup>	$PdCl_2$ <sup>b,c</sup>	$PdCl_2$ <sup>b,d</sup>
<b>g</b>	<i>R</i> <sup>e</sup> $CH_3SCH_2$	38( <i>S</i> )	<i>f</i>	<i>f</i>	<i>f</i>
<b>h</b>	<i>S</i> $CH_3S(CH_2)_2$	65( <i>S</i> )	59( <i>S</i> )	32( <i>S</i> )	<i>f</i>
<b>j</b>	<i>S,S</i> $CH_3S(O)(CH_2)_2$	70( <i>S</i> )	<i>f</i>	<i>f</i>	<i>f</i>
<b>k</b>	<i>S</i> $(CH_3)_2N(CH_2)_4$	58( <i>S</i> )	34( <i>S</i> )	2( <i>S</i> )	<i>f</i>
<b>m</b>	<i>R</i> $CH_3S(CH_2)_3$	70( <i>R</i> )	88( <i>R</i> )	45( <i>R</i> )	35( <i>R</i> )

<sup>a</sup> Ratio ligand/ $Ni$  (or  $Pd$ )  $Cl_2$ /Grignard/vinyl bromide is 1/1/250/125 in  $(C_2H_5)_2O$ ; yields in all cases  $> 90\%$ . <sup>b</sup> Configuration of major enantiomer **3** obtained. <sup>c</sup> Reaction at  $-50^\circ C$  for 4 h followed by 16 h at  $0^\circ C$ . <sup>d</sup> Reaction at  $-10^\circ C$  to  $-5^\circ C$  for 16 h. <sup>e</sup> Ligand derived from *S*-cysteine; in terms of the Cahn-Ingold Prelog rules the configurational symbol changes in the case of **4**. <sup>f</sup> Reaction not carried out.

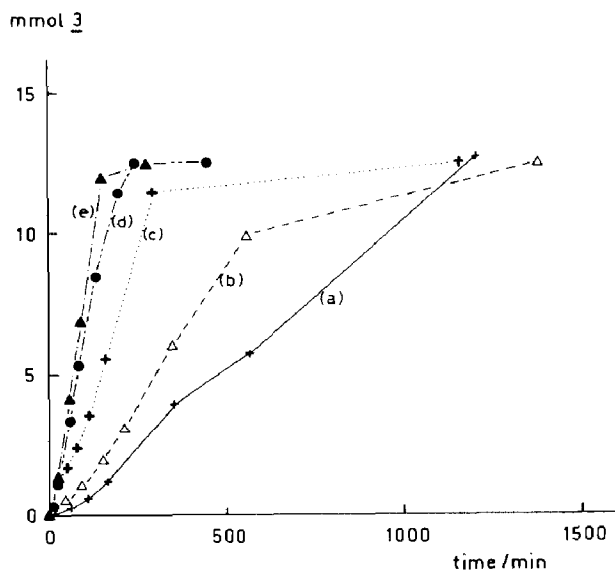


Fig. 5. Rate of formation of **3** in the presence of ligand **4m** and varying amounts of  $\text{ZnBr}_2$ . The maximum theoretical yield of **3** is 12.5 mmol. The code is (a) 0 mol%  $\text{ZnBr}_2$  (rot. **3** +3.60°), (b) 0.13 mol%  $\text{ZnBr}_2$  (rot. **3** +2.20°), (c) 1.0 mol%  $\text{ZnBr}_2$ , (d) 11.5 mol%  $\text{ZnBr}_2$  (rot. **3** -1.83°), (e) 200 mol%  $\text{ZnBr}_2$  (rot. **3** -3.95°). If not reported, the rotation of **3** obtained at the end of the reaction was not measured.

ligands. It does, however, lead to some variation of the e.e.'s for the same ligand, either upwards or downwards depending on the turnover conditions used.

The effect of change of magnesium for other metal ions on the carbanionic component using the readily available ligand **4d** was examined. An equivalent of  $\text{ZnBr}_2$  was added to the Grignard reagent prior to reaction on the assumption that this would produce the dialkylzinc reagent [24\*,25]. The reaction proceeded well, but to our surprise the coupling product **3** turned out to have the *R* rather than *S* configuration normally obtained. This result was thus investigated further.

Reactions were again run under conditions of high turnover on metal/ligand. The Grignard reagent **1** is used in excess (2.5 times more than vinyl bromide) to suppress kinetic resolution of **1**. Details are given in the Experimental Section. The course of the reactions was followed by quantitative GLC, and the amounts of ethylbenzene (from quenched Grignard reagent), **3**, and 2,3-diphenylbutane (two diastereomers, formed during generation of the Grignard reagent from 1-phenylethylchloride) was determined. Aliquots were taken at regular intervals and were quenched in aqueous hydrochloric acid prior to analysis. Reaction was assumed complete when the concentration of **3** no longer changed. The reaction mixture was then worked up, product **3** was isolated, and the optical rotation was determined on neat pure material. The course of several reactions is illustrated graphically in Fig. 5 and the data for reactions with and without  $\text{ZnBr}_2$  (2–2.5 fold excesses) are shown in Table 2.

For ligands **4b**, **4g**, **4h**, **4k**, **4m** the rates increase upon addition of an excess of anhydrous  $\text{ZnBr}_2$ . This is clear both from Table 2 and Fig. 5. There are significant rate differences between the various ligands. The fastest reaction is with **4g** in the presence of  $\text{ZnBr}_2$  (entry 6), but the enantioselectivity is poor (either entry 5 or 6).

Table 2

Effect of added  $\text{ZnBr}_2$  on rates and configuration of **3** with different ligands <sup>a</sup>

Entry	Ligand	$\text{ZnBr}_2$ (mol%) <sup>b</sup>	$t_{1/2}$ (min)	$t_{100}$ (min) <sup>c</sup>	Yield of <b>3</b> (%)	$[\alpha]_D^{22}$ (neat) <sup>d</sup>	Optical yield (configuration)
1	<b>4m</b>	–	600	1200	> 95	+3.60°	61 ( <i>S</i> )
2	<b>4m</b>	250	105	350	> 95	–3.95°	67 ( <i>R</i> )
3	<b>4h</b>	–	265	700	> 95	+3.52°	60 ( <i>S</i> )
4	<b>4h</b>	250	82	275	> 95	–3.08°	52 ( <i>R</i> )
5	<b>4g</b>	–	280	950	> 95	+2.15°	36 ( <i>S</i> )
6	<b>4g</b>	250	50	200	> 95	–0.10°	2 ( <i>R</i> )
7	<b>4k</b>	–	800	2600	> 95	+2.75°	47 ( <i>S</i> )
8	<b>4k</b>	250	(130) <sup>e</sup>	– <sup>c</sup>	38	–2.67°	45 ( <i>R</i> )
9	<b>4b</b>	–	720	1600	> 95	+4.10°	69 ( <i>S</i> )
10	<b>4b</b>	200	140	– <sup>e</sup>	56–78	–2.43°	41 ( <i>R</i> )

<sup>a</sup> Reactions at 0 °C in diethyl ether ratio Ni(ligand)/**2**/1 is 1/100/2500. <sup>b</sup> Relative to vinyl bromide **2**.<sup>c</sup> Time beyond which the concentration of **3** did not increase further. <sup>d</sup>  $[\alpha]_D^{22} = -5.91^\circ$  (neat) is taken as the rotation of optically pure **3**; see ref. 7\* for comments on temperature dependence of rotation.<sup>e</sup> Difficult to ascertain because of sluggish reaction.

What is immediately obvious is a switch in enantioselectivity for every ligand in going from reaction in the absence to that in the presence of  $\text{ZnBr}_2$  (every odd compared with even entry). In all cases in the absence of  $\text{ZnBr}_2$  the *S*-enantiomer of **3** is formed. In the presence of  $\text{ZnBr}_2$  the *R*-enantiomer is produced. It seems reasonable in the case of **4g** (entry 6) to attribute the formation of nearly racemic **3** to the same type of reversal, namely a tendency to form greater amounts of *R*-**3** in the presence of  $\text{ZnBr}_2$ .

In Table 3 are shown details of another series of experiments that provide considerably more insight. From entries 11–14, in which ligands **4b** and **4h** were used, it is clear that the  $\text{ZnBr}_2$ -induced switch occurs also in Pd-catalyzed reactions. These reactions, carried out with preformed  $\text{Pd}^0$ /ligand catalyst (via reduction of  $\text{Pd}^{\text{II}}$ /ligand with DIBAH) are sluggish and, in contrast to the Ni catalyzed reactions, become even more so in the presence of  $\text{ZnBr}_2$ . In entries 15 and 16 the effect of electrophilic  $\text{MgBr}_2$  on the absence of  $\text{ZnBr}_2$  is examined. The effect of  $\text{MgBr}_2$  on the enantioselectivity is at best very small. In the case of entries 17 and 18 the Grignard reagent was treated with one equivalent of  $\text{ZnBr}_2$  and the mixture was allowed to stand for 1 h, after which time the dialkylzinc should be formed [25]. No detectable coupling occurs, which strongly implies that a dialkylzinc is not the reactive intermediate. In the case of ligands **4d** and **4m** (these were the ones examined, but there is no reason to believe that other ligands would behave differently) added anhydrous  $\text{ZnCl}_2$  has a powerful inhibitory effect (entry 19).  $\text{ZnI}_2$  (entries 20 and 22) leads to reversal in enantioselection, but the reaction rates are markedly lower.

The most revealing results shown in Table 3 involve entries 23 and 24, which refer to two reactions, each with ligand **4m**, identical in every respect save that  $\text{ZnBr}_2$  was added in the case of 24. The second important feature is that the reactions were carried out at –35 °C instead of the 0 °C used for all other reactions involved in Table 3. There was virtually no reaction in the absence of  $\text{ZnBr}_2$ , whereas with  $\text{ZnBr}_2$  (entry 24) present there was acceptable yield of product. There

Table 3

Effect of various additives, transition metals, and ligands on the formation of **3**<sup>a</sup>

Entry	Ligand/Metal	Temperature (°C)	Time (h)	Additive <sup>b</sup>	Yield of <b>3</b> (%)	$[\alpha]_D^{22}$	Optical yield (config.)
11	<b>4h</b> /Pd	0	120	–	> 95	+1.92°	33( <i>S</i> )
12	<b>4h</b> /Pd	0	120	ZnBr <sub>2</sub>	12	–1.00°	17( <i>R</i> )
13	<b>4b</b> /Pd	0	120	–	86	+1.87°	32( <i>S</i> )
14	<b>4b</b> /Pd	0	120	ZnBr <sub>2</sub>	< 10	– <sup>c</sup>	– <sup>c</sup>
15	<b>4m</b> /Ni	0	60	MgBr <sub>2</sub>	> 95	+3.49°	59( <i>S</i> )
16	<b>4b</b> /Ni	0	60	MgBr <sub>2</sub>	> 95	+4.35°	74( <i>S</i> )
17	<b>4m</b> /Ni	0	96	ZnBr <sub>2</sub>	nil <sup>d</sup>	–	–
18	<b>4h</b> /Ni	0	16	ZnBr <sub>2</sub>	nil <sup>d</sup>	–	–
19	<b>4b</b> /Ni	0	80	ZnCl <sub>2</sub>	nil	–	–
20	<b>4b</b> /Ni	0	80	ZnI <sub>2</sub>	43	–2.75°	47( <i>R</i> )
21	<b>4m</b> /Ni	0	16	ZnCl <sub>2</sub>	nil	–	–
22	<b>4m</b> /Ni	0	16	ZnI <sub>2</sub>	16	–3.07°	52( <i>R</i> )
23	<b>4m</b> /Ni	–34	20	–	0.4	–	–
24	<b>4m</b> /Ni	–34	21	ZnBr <sub>2</sub>	73	–4.14°	70( <i>R</i> )

<sup>a</sup> Reaction conditions identical to those described in Table 2. <sup>b</sup> Present in 25% excess based on **2**.<sup>c</sup> Insufficient material to determine rotation. <sup>d</sup> The Grignard reagent **1** was allowed to stand for several hours with the zinc halide prior to use. Under these conditions the dialkylzinc reagent is formed and this is not reactive.

seems to be only one tenable conclusion. Two competing reactions are involved, a fast one with ZnBr<sub>2</sub> (with Ni<sup>0</sup> as catalyst), and a slower one involving the Grignard reagent. The stereochemical consequences of these two reactions are opposite.

The reactions listed in Tables 2 and 3 were performed in the presence of an excess of ZnBr<sub>2</sub> (relative to vinyl bromide). In Table 3 the effect of variation in the amount of ZnBr<sub>2</sub> on both rate and optical rotation of **3** are shown. Entries 25 and 26 reveal saturation of the system. There is no advantage in using much more than one equivalent of ZnBr<sub>2</sub> with respect to vinyl bromide. Even 0.11 equivalent (entry 27) of ZnBr<sub>2</sub> (again with respect to vinyl bromide, which is taken as 100 mol%) produces more than a threefold rate increase compared the  $t_{1/2}$  time for entry 29. Significant acceleration is still seen with only 0.13 equivalent (entry 29). The changes in both  $t_{1/2}$  and  $[\alpha]_D$  as a function of  $[\text{ZnBr}_2]/[\text{vinyl bromide}]$  are not linear (plot not shown). The simplest explanation of the changes in both parameters is,

Table 4

Effect of concentration of ZnBr<sub>2</sub> on the formation of **3** catalyzed by Ni<sup>0</sup>/**4e**<sup>a</sup>

Entry	Zn(Br) <sub>2</sub> (mol%) <sup>b</sup>	$t_{1/2}$ (min)	$t_{100}$ <sup>c</sup> (min)	Yield of <b>3</b> (%)	$[\alpha]_D^{22}$
25	100	80	160	> 95	–
26	200	105	250	> 95	–3.95°
27	11	175	400	> 95	–1.83°
28	1.0	380	580	> 95	–
29	0.13	370	750	> 95	+2.20°
30	0.00	600	1200	> 95	+3.60°

<sup>a</sup> Conditions same as described in Table 2. <sup>b</sup> Relative to the limiting reagent vinyl bromide (**2**). <sup>c</sup> Time beyond which the concentration of **3** did not increase further.

Table 5

Effect of ZnBr<sub>2</sub> on the formation of **3** using Ni<sup>0</sup> phosphine ligands <sup>a</sup>

Entry	Ligand	ZnBr <sub>2</sub> (mol%)	<i>t</i> <sub>1/2</sub> (min)	<i>t</i> <sub>100</sub> <sup>b</sup> (min)	Yield (%)
31	<b>15</b>	–	– <sup>c</sup>	– <sup>c</sup>	8
32	<b>15</b>	250	270 <sup>d</sup>	–	68
33	<b>16</b>	–	– <sup>e</sup>	– <sup>e</sup>	0
34	<b>16</b>	250	– <sup>c</sup>	– <sup>c</sup>	6

<sup>a</sup> Reaction conditions identical to Table 2. <sup>b</sup> Time beyond which the concentration of **3** did not increase further. <sup>c</sup> <10% in 600 min. <sup>d</sup> Projection of reaction pathway prior to cessation of product formation. <sup>e</sup> No product in 24 h.

indeed, in terms of two competing reactions with opposite stereochemical outcomes. At more than 100 mol% ZnBr<sub>2</sub> the slower reaction apparently fails to compete effectively.

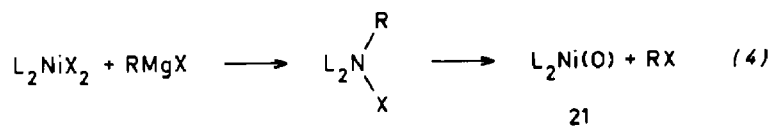
Two simple chiral phosphine ligands, 1,2-diphenylphosphinoethane (**15**), and triphenylphosphine (**16**) were examined (Table 5). Ligand **15** is known to promote at best only very slow cross coupling under the conditions used [24\*]. This was experimentally confirmed (entry 33). Addition of an excess of ZnBr<sub>2</sub> led to formation of detectable amounts of **3** although the accelerating effect was very small (entry 34). Ligand **16**, on the other hand, under these conditions is known to lead to slow but appreciable cross coupling [25]. At 0 °C almost 10% of product formation had occurred after 600 min (entry 31); addition of an excess of ZnBr<sub>2</sub> to the reaction mixture (entry 32) induced an unmistakable increase in the rate of formation of **3**. This indicates that the effect of ZnBr<sub>2</sub> is not directly associated with some special characteristic of the β-aminophosphine ligands.

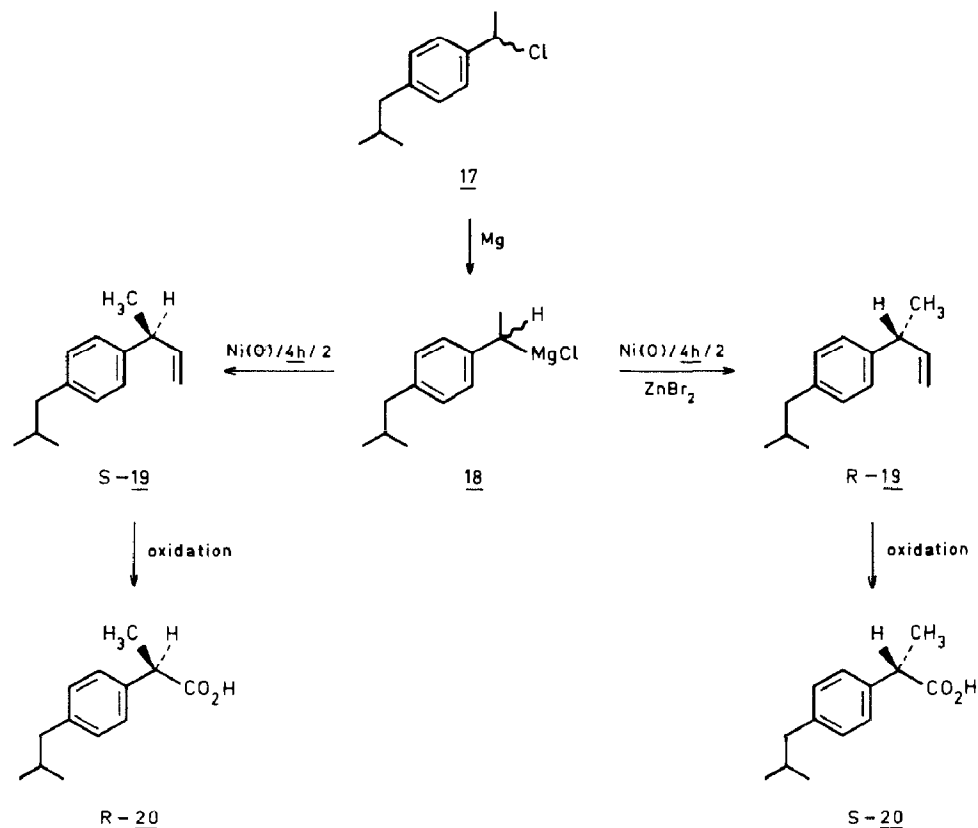
### E. A synthetic application

The ZnBr<sub>2</sub>-induced switch in enantioselectivity opens up the possibility of preparing from a single ligand either enantiomer of a coupling product. The analgesic ibuprofen (**20**) [26] was chosen as a target. The approach used is given in Scheme 5. *R*-**19**, [α]<sub>D</sub><sup>20</sup> –3.44° (neat), was obtained in >95% yield with L-**4h** as ligand and 2.5 equiv. ZnBr<sub>2</sub> whereas *S*-**19**, [α]<sub>D</sub><sup>20</sup> +3.65° (neat), was produced in >95% yield with no added ZnBr<sub>2</sub>. Use of published literature data [5] indicates that the e.e.'s of *R*- and *S*-**19** are 49 and 52%, respectively. The oxidation of **19** to ibuprofen (**20**) without racemization has been described previously [5].

## Discussion

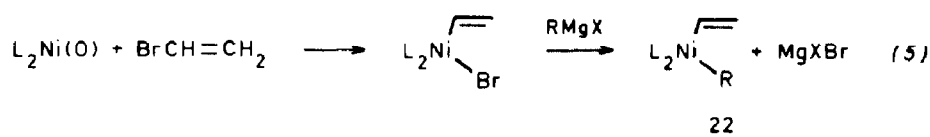
The cross coupling reaction of eq. 1 is a classical example of an oxidative addition/reductive elimination cycle [4c]. In the case of Ni-catalyzed processes the Ni<sup>II</sup> ligand complex is first reduced to Ni<sup>0</sup> intermediate **21** (eq. 4), where L



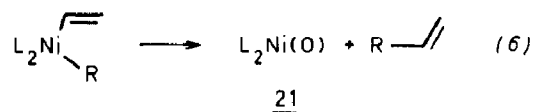


Scheme 5

represents ligand. Oxidative insertion of  $\text{Ni}^0$  into the  $sp^2$  carbon-halogen bond of vinyl bromide, followed by exchange with Grignard reagent, gives **22** (eq. 5).



Reductive elimination from **22** gives the coupling product and regenerates **21** (eq. 6).



The reaction cycle represented by eq. 4–6 can be readily repeated at least 1000 times. An idea of the efficiency of this process can be gained by making comparisons with catalysts of undisputed efficiency. Consider, for example, succinate dehydrogenase, which operates on a substrate, succinic acid, molecular weight (MW) of 118, to give a product, fumarate, of virtually the same molecular weight [27]. Succinate dehydrogenase is not an exceptionally efficient enzyme; it has a turnover of  $1.15 \times 10^3 \text{ min}^{-1}$  and a molecular weight of  $1.05 \times 10^5$ . In the presence of  $\text{ZnBr}_2$  with **4m** as ligand, product **3**, MW 132, is produced with a turnover, as derived from Fig. 5, of about  $10 \text{ min}^{-1}$  from a complex of MW 402. To produce 1

gram  $\text{min}^{-1}$  of product (fumarate for the enzyme, **3** for the organometallic complex) about 0.7 g of enzyme (MW  $1.05 \times 10^4$ ) or 320 g of complex (MW  $4 \times 10^2$ ) would be needed. On this basis the organometallic system does not compare so badly in terms of rate, amounts of material required, or selectivity with a "typical" enzyme.

This relatively high efficiency results, however, in the experimental problem that the intermediates cannot readily be isolated, and mechanistic interpretations necessarily involve considerable speculation. Virtually nothing is known of potential reversibility of various steps nor is the rate limiting process known. There is, however, complete consistency between ligand configuration and the configuration of product obtained. This indicates that the type of coordination and the influence of steric factors are the same for related ligands.

The results with ligand **4m** indicate that e.e.'s can be systematically improved by other than simple steric means. The heteroatom in the side chain clearly participates in reactions that do not involve  $\text{ZnBr}_2$ , perhaps in the manner schematically depicted in eq. 3. Operation of such a mechanism implies that the addition of the Grignard reagent to the Ni-oxidative addition product with vinyl bromide must be reversible, in order to allow selection between the two possible configurations of the chiral benzylic carbon. This reversibility may be more important with **4m**; the e.e. of **3** increases with increasing temperature (Table 1), consistent with a temperature effect on a reversible reaction.

To our knowledge the effect of zinc halides has little precedent. Posner [28] has observed that zinc halides influence the addition of organocopper reagents to  $\alpha,\beta$ -unsaturated sulfoxides. In general for  $\text{Ni}^0$  catalyzed reactions,  $\text{ZnBr}_2$  increases the rate and reverses the direction of enantioselectivity. The kinetic data are consistent with a fast  $\text{Zn}^{\text{II}}$  induced pathway and a slower reaction involving the Grignard reagent. The inhibitory effect of  $\text{ZnCl}_2$  suggests that the rate of some exchange reactions on  $\text{Zn}^{\text{II}}$  is halide dependent, chloride exchanging more slowly. Moreover, the dialkylzinc species, if allowed to form, is apparently not very reactive. The appropriate balance of reactivity may be reached in  $\text{RZnBr}$ , the monoexchanged species. On the other hand, the formation of zincates may also influence the course of the reaction. Only further investigation can provide answers to these questions.

## Experimental

The circular dichroism spectra were recorded on a Jobin Yvon auto dichrograph Mark V with methanol as a solvent in a 1 cm cell. UV spectra were recorded with a Perkin-Elmer Lambda 5 UV/VIS spectrophotometer. Cross couplings were carried out as previously described [6]. The products of the cross-coupling reaction (**3**) and (**19**) were isolated by preparative GLC on a Hewlett Packard F & M 700 gas chromatograph, equipped with a TC detector, using a 8 ft,  $\frac{1}{2}$  inch S.S. column filled with 15% UCCW 982 on Chromosorb W, 30-60 mesh. The purified products were checked for impurities on analytical GLC on a Perkin-Elmer F17 gas chromatograph equipped with a F1 detector, using an analytical S.S. column, 6 ft,  $\frac{1}{8}$  inch, filled with 10% SE 30 on Chromosorb W-AW DMCS 80-100 mesh.

*Dimethylamino acids.* *S*-methionine-(*R*)-*S*-oxide, *S*-lysine, (*S*)-2-amino-6-methylthio-4-thiahexanoic acid, and *R*-homomethionine were hydrogenated in the pres-

ence of formaldehyde as previously described [29]. The crude, dried, *N,N*-dimethylamino acids were reduced without recrystallization.

(*S*)-2-Dimethylamino-4-methylthio-1-butanol was prepared in 75% yield from (*S*)-methionine as previously described [6];  $[\alpha]_D^{20} + 37.5^\circ$  (*c* 1.2, CH<sub>2</sub>Cl<sub>2</sub>) [lit. [17]  $[\alpha]_D^{20} + 35.0^\circ$  (*c* 1.1, CH<sub>2</sub>Cl<sub>2</sub>)]. A sample of the alcohol (20 mg) and Eu(hfc)<sub>3</sub> in CDCl<sub>3</sub> was examined by <sup>1</sup>H NMR. Compared with the signal from the alcohol in the absence of Eu(hfc)<sub>3</sub>, the N(CH<sub>3</sub>)<sub>2</sub> resonance was shifted by 3.85 ppm downfield and the SCH<sub>3</sub> resonance by 0.5 ppm downfield. For racemic alcohol two N(CH<sub>3</sub>)<sub>2</sub> singlets will the same integration, separated by 0.22 ppm, and two SCH<sub>3</sub> singlets, separated by 0.07 ppm, were observed in the presence of Eu(hfc)<sub>3</sub>. Addition of 5 mg of racemic alcohol to optically pure alcohol (20 mg) gave rise to new peaks in the calculated ratio.

Similar experiments were performed to establish the enantiomeric purities of the other amino alcohols described. No racemization was observed within the limits of NMR accuracy.

(*S*)-2,6-Bis(dimethylamino)-1-hexanol was prepared in 70% yield from (*S*)-lysine; b.p. (Kugelrohr) 140°C (0.01 Torr); <sup>1</sup>H NMR (CDCl<sub>3</sub>): δ 1.1–1.6 (m, 6H), 2.20 (s, 6H), 2.26 (s, 6H), 2.2–2.6 (m, 3H), 3.25 (dd, 1H, *J* 10 Hz and 9 Hz, one of CH<sub>2</sub>OH), 3.50 (dd, 1H, *J* 10 Hz and 5 Hz, one of CH<sub>2</sub>OH), 4.12 (s, 1H, CH<sub>2</sub>OH);  $[\alpha]_D^{20} + 10.8^\circ$  (*c* 4.11, EtOH) [lit. [30]  $[\alpha]_D^{20} + 9.8^\circ$  (*c* 2.23, EtOH)].

(*S*)-2-Dimethylamino-6-methylthio-4-thia-hexanol. The reported procedure [31] for (*S*)-alkyl cysteine derivatives was used to prepare (*S*)-2-amino-6-methylthio-4-thiahexanoic acid from (*S*)-cysteine and 2-chloroethyl methyl sulfide. After hydrogenation in the presence of formaldehyde [29] the dimethylamino acid was reduced as previously described [6]. Overall yield from (*S*)-cysteine was 58%; b.p. (Kugelrohr) 160°C (0.01 mmHg); <sup>1</sup>H NMR (CDCl<sub>3</sub>): δ 2.1 (s, 3H), 2.3 (s, 6H), 2.5 (m, 3H), 2.7 (s, 4H), 2.95 (m, 2H), 3.5 (m, 1H); <sup>13</sup>C NMR (CDCl<sub>3</sub>): δ 63.8 (d), 59.3 (t), 39.5 (q), 32.9 (t), 31.2 (t), 27.0 (t), 14.4 (q);  $[\alpha]_D^{23} + 2.12^\circ$  (1 cm, neat); mass spectrum, exact mass *m/e* 209.088 (theory 209.091).

(*R*)-2-Dimethylamino-5-methylthio-1-pentanol. This was prepared from D-homomethionine in 72% yield; b.p. (Kugelrohr) 115°C (0.05 Torr); <sup>1</sup>H NMR (CDCl<sub>3</sub>): δ 1.6 (m, 4h), 2.0 (s, 3H), 2.2 (s, 6H), 2.3 (m, 3H), 3.3 (m, 3H);  $[\alpha]_D^{20} - 27.3^\circ$  (*c* 1.74, CH<sub>2</sub>Cl<sub>2</sub>).

(*S*)-2-Dimethylamino-4-methylthio-(*R*)-*S*-oxide-1-butanol. The reported procedure [17] was modified in the reduction step because otherwise too much sulfoxide is reduced. The reduction was carried out under nitrogen for 2 h at -10°C, 2 h at 0°C, and 1 h at room temperature, and monitored by IR spectroscopy; yield 52% from the ester, m.p. 65.5–67°C (lit. [31], 58–61°C); <sup>13</sup>C NMR (CDCl<sub>3</sub>): δ 63.6 (d), 60.1 (t), 51.2 (t), 40.1 (q), 37.9 (q), 18.6 (t);  $[\alpha]_D^{21} + 111.8^\circ$  (*c* 1.0, CH<sub>2</sub>Cl<sub>2</sub>) [lit. [31]  $[\alpha]_D^{20} + 100.4^\circ$  (*c* 1.04, CH<sub>2</sub>Cl<sub>2</sub>)].

*Preparation of diphenylphosphine derivatives 4.* A dry 250 ml three-necked flask was charged with a stirring bar the alcohol (10 mmol), 75 ml of freshly distilled THF, and triethylamine (11 mmol) and was kept filled with nitrogen. The solution was cooled to 0°C, and methanesulfonyl chloride in 25 ml of dry THF was added dropwise in about 5 min. The mixture was stirred for 2 h at 0°C and then treated in one portion, with the deep red mixture obtained from (C<sub>6</sub>H<sub>5</sub>)<sub>2</sub>PH (purchased from Alfa) (10 mmol) and KOC(CH<sub>3</sub>)<sub>3</sub> (2.8 g, 25 mmol) in 50 ml of freshly distilled THF, at 0°C. The deep red color faded immediately to give a thick, orange-yellow



mixture, which was stirred for an additional 2 h at 0°C. At the end of this period the color mixture was yellow. After evaporation of the solvent, the residue was shaken with 50 ml of 15% NaOH and 50 ml of benzene, and the aqueous layer separated and extracted twice more with 50 ml portions of benzene. The organic fractions were combined, washed with brine, dried quickly over MgSO<sub>4</sub>, and evaporated. Kugelrohr distillation (0.003 Torr) gave a small fraction of unchanged alcohol at 100–110°C, followed by the desired phosphine, which distilled at 180–200°C.

(*S*)-2-Dimethylamino-1-diphenylphosphino-4-methylthiobutane (**4h**), (*S*)-methphos was obtained in 80% yield; b.p. (Kugelrohr) 180–190°C (0.001 Torr); <sup>1</sup>H NMR (CDCl<sub>3</sub>): δ 1.76 (m, 2H), 2.00 (s, 3H), 2.11 (s, 6H), 2.30 (m, 1H), 2.52 (m, 4H), 7.25 (m, 10H); <sup>13</sup>C NMR (CDCl<sub>3</sub>): δ 139.0 (t), 133.0 (d), 132.3 (d), 128.4 (d), 128.0 (d), 59.8 (d), 39.6 (s), 31.4 (s), 30.8 (d), 27.4 (d), 15.2 (s); mass spectrum, *m/e* 132 (100%), 256 (4.3%), 316 (16.7%) (a methyl group fragments from the parent molecular ion); [α]<sub>D</sub><sup>21</sup> – 69.2° (*c* 1.1, CHCl<sub>3</sub>). Anal. Calcd for C<sub>19</sub>H<sub>26</sub>NPS: C 68.85, H 7.91, N 4.23, P 9.34, S 9.67; found: C 68.92, H 7.98, N 4.34, P 9.61, S 9.5.

(*S*)-2-Dimethylamino-1-diphenylphosphino-4-methylthio-(*R*)-*S*-oxidebutane (**4j**), (*S*),(*S*)-methphossulfoxide was obtained in 46% yield after purification by column chromatography on closely packed Al<sub>2</sub>O<sub>3</sub> with ether and ether/methanol (19:1) as eluent; <sup>1</sup>H NMR (CDCl<sub>3</sub>): δ 1.83 (m, 3H), 2.14 (s, 6H), 2.42 (m, 2H), 2.50 (s, 3H), 2.71 (m, 2H), 7.40 (m, 10H); [α]<sub>D</sub><sup>22</sup> + 37.0° (*c* 0.65, benzene); mass spectrum, exact mass *m/e* 347.149 (theory 347.147).

(*S*)-2,6,-Bis(dimethylamino)-1-diphenylphosphino-hexane (**4k**), (*S*)-lysphos was obtained in 75% yield b.p. (Kugelrohr) 190°C (0.03 Torr); <sup>1</sup>H NMR (CDCl<sub>3</sub>): δ 1.34 (m, 6H), 2.20 (s, 6H), 2.21 (s, 6H), 2.25 (m, 5H), 7.17 (m, 10H); [α]<sub>D</sub><sup>20</sup> – 39.2° (*c* 1.8, CHCl<sub>3</sub>); mass spectrum, *m/e* 341 (parent minus a methyl group).

(*R*)-2-Dimethylamino-1-diphenylphosphino-5-methylthiopentane (**4m**, (*R*)-homomethphos) was obtained in 65% yield; b.p. (Kugelrohr) 190–200°C (0.01 Torr); <sup>1</sup>H NMR (CDCl<sub>3</sub>): δ 1.60 (m, 4H), 2.00 (s, 3H), 2.11 (s, 6H), 2.25 (br, m, 5H), 7.20 (m, 10H); [α]<sub>D</sub><sup>20</sup> + 52.9° (*c* 1.36, CHCl<sub>3</sub>); mass spectrum, *m/e* 146 (100%), 345 (parent, 0.5%). Anal. Calcd for C<sub>20</sub>H<sub>28</sub>NPS: C 69.53, H 8.17, N 4.05; found: C 68.99, H 8.09, N 3.99.

*Preparation of palladium complexes.* To a stirred suspension of bis(benzonitrile)-palladium(II) chloride (383.5 mg, 1 mmol) in 9 ml of benzene under nitrogen was added a solution of 1 mmol of the phosphine ligand in 15 ml of benzene. The mixture was kept overnight at room temperature and the yellow precipitate then filtered off, (P4 glass filter), washed with benzene, and dried in vacuo.

PdCl<sub>2</sub>[(*S*)-Methphos (**21d**)] was obtained in 70% yield after recrystallization from CH<sub>2</sub>Cl<sub>2</sub>/hexane; m.p. 244–246°C (dec.); <sup>1</sup>H NMR (CD<sub>2</sub>Cl<sub>2</sub>): δ 1.67 (br s, 2H), 2.02 (s, 3H), 2.40 (m, 1H), 2.60 (br, m, 4H), 2.97 (s, 3H), 3.12 (s, 3H), 7.60 (br, m, 8H), 8.0 (m, 2H); [α]<sub>D</sub><sup>20</sup> – 52.8° (*c* 0.72, CH<sub>2</sub>Cl<sub>2</sub>). Anal. Calcd for C<sub>19</sub>H<sub>26</sub>Cl<sub>2</sub>NPSPd; C 44.85, H 5.15, N 2.75, S 6.30; found: C 44.71, H 5.12, N 2.83, S 6.29.

PdCl<sub>2</sub>[(*S*)-Lysphos (**4k**)] was obtained in 75% yield on precipitation from benzene; m.p. 135–138°C; <sup>1</sup>H NMR (CD<sub>2</sub>Cl<sub>2</sub>): δ 1.38 (br, m, 6H), 2.18 (s, 6H), 2.5–2.7 (br, m, 5H), 2.99 (s, 3H), 3.15 (s, 3H), 7.70 (br, m, 8H), 8.10 (m, 2H); [α]<sub>D</sub><sup>20</sup> – 61.2° (*c* 0.42, CH<sub>2</sub>Cl<sub>2</sub>).

PdCl<sub>2</sub>[(*R*)-Homomethphos (**4m**)] was obtained in 60% yield after recrystallization

from acetonitrile; m.p. 144–146 °C;  $^1\text{H NMR}$  ( $\text{CD}_2\text{Cl}_2$ ):  $\delta$  1.63 (br, m, 4H), 2.05 (s, 3H), 2.3–2.8 (br, m, 5H), 2.93 (s, 3H), 3.10 (s, 3H), 7.55 (br, m, 8H), 8.05 (m, 2H);  $[\alpha]_{\text{D}}^{20} + 56.9^\circ$  (c 0.46,  $\text{CH}_2\text{Cl}_2$ ).

*Racemic homomethionine (13)*. Diethyl acetamidomalonate (86.8 g, 400 mmol) was added to a warm solution of 9.2 g of sodium (400 mmol) in 500 ml of ethanol (abs) under nitrogen. After 15 min stirring, the mixture was cooled to 10 °C and 48 g (400 mmol) of allyl bromide was slowly added (exothermic reaction). The mixture was stirred and warmed for 30 min, then evaporated to dryness, and 200 ml of  $\text{H}_2\text{O}$  and 200 ml of  $\text{CHCl}_3$  were added and the  $\text{CHCl}_3$  layer separated. The aqueous layer was extracted twice more with 100 ml of  $\text{CHCl}_3$ . The  $\text{CHCl}_3$  fractions were combined, washed with brine, and dried over  $\text{MgSO}_4$ . After filtration and evaporation a nearly quantitative yield of  $\alpha$ -allylated product was obtained;  $^1\text{H NMR}$  ( $\text{CDCl}_3$ ):  $\delta$  1.27 (t, 6H), 2.05 (s, 3H), 3.07 (d, 2H), 4.17 (q, 4H), 4.8–5.8 (br, m, 3H), 6.73 (br, s, 1H). Half of this amount, 200 mmol, was added to a mixture of 50 ml of ethanol, benzoyl peroxide (500 mg), and mercuric acetate (2.25 g). A nitrogen atmosphere was introduced, and cooled to  $-30^\circ\text{C}$ . Methanethiol (15 ml) was quickly added and the whole mixture was irradiated with a high-pressure mercury lamp (Hanau TQ-150) with a quartz filter for one night at  $-10^\circ\text{C}$ . The resulting black mixture was filtered and the solvent was evaporated, affording 95% crude product of addition of methanethiol;  $^1\text{H NMR}$  ( $\text{CDCl}_3$ ):  $\delta$  1.27 (t, 6H), 1.35 (m, 2h), 2.05 (s, 6H,  $\text{CH}_3\text{S}$  and  $\text{COCH}_3$ ), 2.37 (m, 4H), 4.17 (q, 4H), 6.75 (br, s, 1H). To this crude material was added 200 ml of 4N hydrochloric acid, and the mixture was refluxed for 6 h. The clear solution formed was evaporated to dryness and 100 ml of  $\text{H}_2\text{O}$  was added. With cooling and stirring, 10 M aqueous NaOH was carefully added to pH 7. The white solid obtained was filtered off on a P3 glass filter and dried, to give 75% yield of racemic homomethionine (**13**);  $^1\text{H NMR}$  ( $\text{D}_2\text{O}/\text{DCl}$ ):  $\delta$  1.70 (m, 2H), 1.92 (m, 2H), 2.00 (s, 3H), 2.52 (t, 2H), 4.08 (t, 1H).

*Racemic homomethionine amide*. To a mixture of **13** (16.3 g, 100 mmol) in 100 ml of  $\text{CH}_3\text{OH}$ , a solution of  $\text{SOCl}_2$  (17.8 g, 150 mmol) was added dropwise; the temperature was kept at 5 °C. When addition was complete, the mixture was refluxed for 1 h. After cooling, and evaporation of the solvent, 150 ml of  $\text{H}_2\text{O}$  and 150 ml of  $\text{CHCl}_3$  were added to the crude ester. With stirring and cooling, the mixture was made basic (pH 10) with 10 M NaOH. The  $\text{CHCl}_3$  layer was separated and the water layer was extracted twice more with  $\text{CHCl}_3$ . The combined  $\text{CHCl}_3$  fractions were washed with brine, and dried over  $\text{MgSO}_4$ . After evaporation of the solvent, the amino ester was used without further purification.  $^1\text{H NMR}$  ( $\text{CDCl}_3$ ):  $\delta$  1.50 (br, 2, 2H), 1.70 (m, 4H), 2.00 (s, 3H), 2.47 (m, 2H), 3.43 (m, 1H), 3.63 (s, 3H). Aqueous ammonia (25%) (60 ml) was added to the ester, the mixture was stirred overnight at room temperature, and the solvent then evaporated. After addition of 50 ml of dry  $\text{CHCl}_3$ , the mixture was filtered, dried over  $\text{MgSO}_4$ , and again filtered. After evaporation of the  $\text{CHCl}_3$ , the resulting crude amide crystallized in 70% yield on standing;  $^1\text{H NMR}$  ( $\text{CDCl}_3$ ):  $\delta$  1.30–1.95 (br, m, 6H), 2.00 (s, 3H), 2.47 (m, 2H), 3.30 (m, 1H), 6.70 (br, d, 2H). It was not purified further.

*Resolution of the amide with Pseudomonas putida*. A suspension of DL-homomethionine amide (32.4 g, 200 mmol) in 300 ml of water was kept for 20 h at 40 °C in the presence of the amino peptidase from *Pseudomonas putida* (0.75 g). Benzaldehyde (12 ml) was then added, and the mixture was stirred for 3 h at 30 °C, and the insoluble Schiff base of the unreacted *R*-amide (19.5 g, 78 mmol) was filtered

off;  $[\alpha]_{\text{D}}^{20} + 26.0^{\circ}$  ( $c$  1,  $\text{CH}_3\text{OH}$ );  $^1\text{H}$  NMR ( $\text{DMSO-}D_6$ ):  $\delta$  1.52 (m, 2H), 1.88 (m, 2H), 2.00 (s, 3H), 2.48 (t, 2H), 3.80 (m, 1H), 7.20 (d, 2H), 7.52 (m, 3H), 7.88 (m, 2H), 8.40 (s, 1H);  $^{13}\text{C}$  NMR ( $\text{DMSO-}D_6$ ):  $\delta$  172.8, 161.6, 135.2, 130.4, 128.0, 127.2, 72.0, 32.0, 24.0, 13.6. The filtrate was evaporated and then stirred with  $\text{CH}_3\text{OH}$  (200 ml). S-13 (15.2 g, 93 mmol, 93% yield) was isolated by filtration;  $[\alpha]_{\text{D}}^{20} + 24.7^{\circ}$  ( $c$  0.3, 6  $N$  HCl). The amino acid was shown to be over 95% enantiomerically pure by thin-layer chromatography on silica gel impregnated with a chiral phase (Chiral plate, Machery-Nagel, Dueren) against racemic homomethionine. The insoluble Schiff base (18 g, 72 mmol) was hydrolyzed (27 ml 96%  $\text{H}_2\text{SO}_4$  in 300 ml of  $\text{H}_2\text{O}$ ). There was obtained 8 g (49 mmol, 68% yield) or *R*-13,  $[\alpha]_{\text{D}}^{25} - 25.9^{\circ}$  ( $c$  0.3, 6  $N$  HCl), which is > 99% enantiomerically pure as judged by TLC.

*Resolution of homomethionine with chiral phosphoric acid 12.* A solution of (+)-12 (54 mmol) and racemic 13 (54 mmol) was made up in 150 ml of warm  $\text{H}_2\text{O}/\text{C}_2\text{H}_5\text{OH}$  (2.7:1 v:v). The solution was, stirred for 3 days then filtered to remove solid salt, which was washed with  $\text{H}_2\text{O}$  and dried. This salt then was stirred for 20 h with 130 ml of 2.4  $N$  hydrochloric and the solid (+)-12 was filtered off, and the filtrate was evaporated to dryness and then dissolved in 30 ml of  $\text{H}_2\text{O}/\text{C}_2\text{H}_5\text{OH}$  (1:1 v:v), and the solution neutralized with NaOH solution. The precipitate of 13 was filtered off, washed, and dried to give pure *R*-13 (10 mmol, 37%

Table 6

Atomic coordinates for **4h**·PdCl<sub>2</sub>, with esd in parentheses

Atom	x	y	z	$B$ ( $\text{\AA}^2$ ) <sup>a</sup>
Pd	0.83743(6)	0.245	0.97641(7)	3.18(1)
Cl1	1.0796(3)	0.1988(3)	0.9423(3)	6.14(7)
Cl2	0.9778(3)	0.3701(2)	1.1172(4)	5.71(7)
B	0.1246(4)	0.1440(3)	0.5186(6)	8.3(1)
P	0.6078(2)	0.2829(2)	1.0063(2)	2.82(4)
N	0.6984(8)	0.1265(5)	0.8533(8)	3.1(2)
C1	0.483(1)	0.1779(6)	0.945(1)	3.1(2)
C2	0.509(1)	0.1377(6)	0.803(1)	2.9(2)
C3	0.772(1)	0.0511(7)	0.976(1)	4.4(3)
C4	0.722(1)	0.1036(9)	0.702(1)	4.5(2)
C5	0.411(1)	0.0486(7)	0.748(1)	3.8(2)
C6	0.212(1)	0.0615(8)	0.678(2)	5.2(3)
C7	0.185(2)	0.100(2)	0.369(2)	10.2(7)
C8	0.616(1)	0.3064(6)	1.204(1)	3.0(2)
C9	0.464(1)	0.3203(7)	1.216(1)	3.5(2)
C10	0.462(1)	0.3325(8)	1.367(1)	4.4(2)
C11	0.617(1)	0.3297(9)	1.509(1)	5.1(3)
C12	0.765(1)	0.3129(9)	1.498(1)	5.0(3)
C13	0.770(1)	0.3024(8)	1.348(1)	4.3(3)
C14	0.486(1)	0.3709(7)	0.867(1)	4.4(2)
C15	0.573(1)	0.4509(7)	0.861(1)	4.4(2)
C16	0.476(2)	0.5172(8)	0.747(1)	5.6(3)
C17	0.301(2)	0.5083(9)	0.652(1)	6.3(3)
C18	0.223(2)	0.432(1)	0.661(1)	6.1(3)
C19	0.307(2)	0.3598(9)	0.768(1)	5.4(3)

<sup>a</sup> Anisotropically refined atoms are given in the form of the isotropic equivalent thermal parameter defined as:  $\frac{1}{3}[a^2B_{1,1} + b^2B_{2,2} + c^2B_{3,3} + ab(\cos \gamma) \times B_{1,2} + ac(\cos \beta) \times B_{1,3} + bc(\cos \alpha) \times B_{2,3}]$ .

yield);  $[\alpha]_{\text{D}}^{25} - 23.9^\circ$  ( $c$  0.3, 6N HCl). No attempt was made to isolate more **13** from the solution.

### Structure determination

#### Crystal data for $4h \cdot \text{PdCl}_2$ .

$\text{C}_{19}\text{H}_{26}\text{Cl}_2\text{NPSPd}$ , MW 508.77, space group  $P2_1$ ,  $Z = 2$ ,  $a$  8.740(1),  $b$  14.912(5),  $c$  9.112(2) Å,  $D_c$  1.5829 g · cm<sup>-3</sup>,  $V$  1067.7 Å<sup>3</sup>,  $\lambda$  1.5428 Å,  $\mu$  (Cu- $K_\alpha$ ) 111.9 cm<sup>-1</sup>,  $F(000)$  516.

Data were obtained with a Nonius CAD 4 SDP23M diffractometer, interfaced to a PDP-11/23, graphite monochromated Cu- $K_\alpha$  radiation,  $\omega$ - $2\theta$  scan,  $1^\circ \leq \theta \leq 74^\circ$ , 2240 unique reflections, 2163 reflections with  $I \geq 3\sigma(I)$ , 16 reflections with  $16^\circ \leq \theta \leq 36^\circ$  used to refine cell parameters, crystal dimension 0.15 × 0.15 × 0.23 mm. The heavy Pd atom was found by direct methods (MULTAN 82) [32]. The other non-hydrogen atoms were located from succeeding difference maps. Full matrix least-squares of  $F$  converged to a final  $R = 0.041$  and  $R_{\text{fw}} = 0.046$  ( $w = 1$ ), respectively using anisotropic temperature factors. No attempts were made to locate the hydrogen atoms. Absorption corrections were applied. All computations were performed using CAD4SDP programs.

Positional parameters are given in Table 6, bond angles in Table 7, and bond distances in Table 8.

#### Crystal data for $4m \cdot \text{PdCl}_2$

$\text{C}_{20}\text{H}_{28}\text{Cl}_2\text{NPSPd}$ , MW 522.8, space group  $P2_12_12_1$ ,  $Z = 4$ ,  $a$  6.482(3),  $b$  12.816(1),  $c$  26.990(4) Å,  $D_c$  1.549 g cm<sup>-3</sup>,  $V$  2242.1 Å<sup>3</sup>,  $\lambda$  0.7101 Å,  $\mu$  (Mo- $K_\alpha$ ) 12.22 cm<sup>-1</sup>,  $F(000)$  1064.

Table 7

Bond angles (°) in  $4h \cdot \text{PdCl}_2$ <sup>a</sup>

Cl1-Pd-Cl2	91.1(1)	C2-C5-C6	112.6(8)
Cl1-Pd-P	177.9(1)	S-C6-C5	114.1(8)
Cl1-Pd-N	91.5(2)	P-C8-C9	118.8(6)
Cl2-Pd-P	90.82(9)	P-C8-C13	121.7(7)
Cl2-Pd-N	176.7(2)	C9-C8-C13	119.2(8)
P-Pd-N	86.5(2)	C8-C9-C10	121.2(8)
Pd-P-C1	101.0(3)	C9-C10-C11	119.0(9)
C6-S-C7	101.9(8)	C10-C11-C12	119.9(9)
C1-P-C8	103.1(4)	C11-C12-C13	121.8(9)
C1-P-C14	108.2(4)	C8-C13-C12	118.9(9)
C8-P-C14	108.2(4)	P-C14-C15	118.1(7)
C2-N-C3	111.0(6)	P-C14-C19	120.3(7)
C2-N-C4	108.5(7)	C15-C14-C19	121.6(9)
C3-N-C4	108.5(7)	C14-C15-C16	117.0(1)
P-C1-C2	107.6(5)	C15-C16-C17	122.0(1)
N-C2-C1	109.6(7)	C16-C17-C18	119.0(1)
N-C2-C5	112.3(7)	C17-C18-C19	124.0(1)
C1-C2-C5	110.4(7)	C14-C19-C18	116.0(1)

<sup>a</sup> Numbers in parentheses are estimated standard deviations of the least significant digits.

Table 8

Bond lengths in  $4h \cdot PdCl_2^a$ 

Pd–Cl1	2.370(2)	S–P	5.294(4)
Pd–Cl2	2.293(3)	S–P	5.044(4)
Pd–S	5.977(3)	S–N	5.561(8)
Pd–S	5.927(5)	S–N	5.761(8)
Pd–S	4.703(4)	S–N	4.597(7)
Pd–P	2.214(2)	S–C1	5.776(9)
Pd–N	2.158(7)	S–C1	3.808(9)
Pd–C1	3.145(8)	P–N	2.996(7)
Pd–C1	5.861(7)	P–C1	1.849(9)
Cl1–Cl2	3.329(4)	N–C1	2.490(10)
Cl1–S	4.134(6)	N–C2	1.521(10)
Cl1–S	5.152(6)	N–C3	1.515(12)
Cl1–P	4.583(3)	N–C4	1.522(11)
Cl1–P	4.570(3)	N–C2	1.526(12)
Cl1–N	3.428(7)	C2–C5	1.542(12)
Cl1–N	5.911(7)	C5–C6	1.583(15)
Cl1–C1	5.321(8)	C8–C9	1.399(11)
Cl1–C1	3.532(8)	C8–C13	1.407(12)
Cl1–C1	3.532(8)	C9–C10	1.390(12)
Cl2–S	4.720(6)	C10–C11	1.412(15)
Cl2–P	4.210(3)	C11–C12	1.36(2)
Cl2–N	4.449(7)	C12–C13	1.398(14)
Cl2–C1	4.840(9)	C13–C15	1.431(13)
Pd–Cl1	2.370(2)	C14–C19	1.428(13)
Pd–Cl2	2.293(3)	C15–C16	1.41(2)
Pd–P	2.214(2)	C16–C17	1.40(2)
Pd–N	2.158(7)	C17–C18	1.34(2)
P–C1	1.849(9)	C18–C19	1.43(2)
S–C6	1.800(14)		
S–C7	1.79(2)		
P–C1	1.849(9)		
P–C8	1.806(8)		
P–C14	1.812(9)		

<sup>a</sup> Numbers in parentheses are estimated standard deviations in the least significant digits.

Data were obtained on the apparatus described above with graphite monochromated Mo- $K_\alpha$  radiation,  $\omega$ - $2\theta$  scan,  $1^\circ \leq \theta \leq 35^\circ$ , 5543 unique reflections, 2691 reflections with  $I \geq 3\sigma(I)$ , 25 reflections with  $8.6^\circ \leq \theta \leq 11.4^\circ$  used to refine unit cell parameters, crystal dimensions  $0.35 \times 0.25 \times 0.058$  mm. The heavy Pd atom was found by direct methods (MULTAN) [32]. The other non-hydrogen atoms were revealed from succeeding difference maps. Attempts to locate hydrogen atoms failed. Full matrix least-squares of  $F$  converged to a final  $R = 0.063$  and  $R_{fw} = 0.096$  (for  $w = 1$ ) respectively, using anisotropic factors. Absorption corrections were applied.

Positional parameters are given in Table 9, bond angles in Table 10, and bond distances in Table 11.

Full structural details are available from the senior author (RMK).

Table 9

Atomic coordinates with esd in parentheses

Atom	<i>x</i>	<i>y</i>	<i>z</i>	<i>B</i> (Å <sup>2</sup> ) <sup>a</sup>
Pd	0.0961(2)	−0.00719(8)	0.30032(3)	1.95(1)
Cl1	0.2017(7)	−0.0152(4)	0.2162(1)	3.68(8)
Cl2	0.3342(8)	−0.1309(4)	0.3222(1)	3.26(7)
S	0.341(1)	0.4503(4)	0.4171(2)	4.2(1)
P	−0.0272(6)	−0.0116(3)	0.37601(9)	2.12(5)
N	−0.123(2)	0.1120(9)	0.2858(3)	2.3(2)
C1	−0.254(2)	0.071(1)	0.3708(4)	2.4(2)
C2	−0.209(2)	0.159(1)	0.3336(4)	2.2(2)
C3	−0.024(3)	0.199(1)	0.2586(5)	3.3(3)
C4	−0.287(3)	0.066(2)	0.2534(5)	3.6(3)
C5	0.600(4)	0.225(1)	0.3265(5)	3.0(3)
C6	0.558(3)	0.295(1)	0.3729(5)	3.3(3)
C7	0.386(4)	0.370(1)	0.3622(5)	3.6(3)
C8	0.181(4)	0.552(2)	0.3914(7)	5.4(5)
C9	0.136(3)	0.039(1)	0.4254(4)	2.6(3)
C10	0.299(2)	−0.019(2)	0.4422(4)	3.1(3)
C11	0.422(3)	0.014(2)	0.4809(4)	3.2(3)
C12	0.377(3)	0.110(1)	0.5039(5)	3.4(3)
C13	0.224(4)	0.170(2)	0.4861(6)	4.3(4)
C14	0.096(4)	0.136(1)	0.4476(5)	3.8(3)
C15	−0.113(3)	−0.136(1)	0.3995(4)	3.1(3)
C16	−0.188(3)	−0.211(1)	0.3643(5)	3.2(3)
C17	−0.281(4)	−0.301(2)	0.3816(6)	4.4(5)
C18	−0.300(4)	−0.319(2)	0.4327(6)	3.8(4)
C19	−0.231(4)	−0.246(2)	0.4666(6)	4.6(4)
C20	−0.138(3)	−0.152(1)	0.4504(5)	3.3(3)

<sup>a</sup> Anisotropically refined atoms are given in the form of the isotropic equivalent thermal parameter defined as:  $\frac{1}{3}[a^2B_{1,1} + b^2B_{2,2} + c^2B_{3,3} + ab(\cos \gamma) \times B_{1,2} + ac(\cos \beta) \times B_{1,3} + bc(\cos \alpha) \times B_{2,3}]$ .

Table 10

Bond angles (°) in **4m**·PdCl<sub>2</sub><sup>a</sup>

Cl1–Pd–Cl2	91.3(2)	P–C9–C10	120.0(1)
Cl1–Pd–P	173.9(2)	P–C9–C14	121.0(1)
Cl1–Pd–N	92.7(3)	C10–C9–C14	119.0(2)
Cl2–Pd–P	89.3(1)	C9–C10–C11	122.0(2)
Cl2–Pd–N	175.5(3)	C10–C11–C12	119.0(2)
P–Pd–N	86.9(3)	C11–C12–C13	120.0(2)
Pd–P–C1	102.0(4)	C12–C13–C14	122.0(2)
C7–S–C8	100.8(9)	C9–C14–C13	119.0(2)
C1–P–C9	108.7(7)	P–C15–C16	118.0(1)
C1–P–C15	106.9(9)	P–C15–C20	121.0(1)
C9–P–C15	103.8(7)	C16–C15–C20	121.0(2)
C2–N–C3	106.0(1)	C15–C16–C17	119.0(1)
C2–N–C4	113.0(1)	C16–C17–C18	121.0(2)
C3–N–C4	108.0(1)	C17–C18–C19	120.0(2)
P–C1–C2	109.0(1)	C18–C19–C20	121.0(2)
N–C2–C1	109.0(1)	C15–C20–C19	118.0(2)
C5–C6–C7	110.0(1)		
S–C7–C6	109.0(1)		

<sup>a</sup> Numbers in parentheses are estimated standard deviations in the least significant digits.

Table 11

Bond distances (Å) in  $4m \cdot PdCl_2$  <sup>a</sup>

Pd-Pd	6.482(1)	P-C1	1.82(2)
Pd-Pd	6.482(1)	S-C7	1.83(2)
Pd-Cl1	6.227(5)	S-C8	1.81(3)
Pd-Cl1	2.374(3)	P-C1	1.82(2)
Pd-Cl2	5.220(5)	P-C9	1.822(14)
Pd-Cl2	2.289(5)	P-C15	1.80(2)
Pd-Cl2	6.478(5)	S-S	6.482(9)
Pd-P	2.194(3)	S-S	6.482(9)
Pd-P	6.039(4)	S-P	6.479(7)
Pd-N	2.121(13)	S-P	5.704(5)
Pd-N	5.303(14)	S-N	6.356(13)
Pd-N	5.409(11)	S-N	6.024(11)
Cl1-Cl1	6.482(7)	P-P	6.482(5)
Cl1-Cl1	6.482(7)	P-P	6.482(5)
Cl1-Cl2	6.481(7)	P-N	2.970(10)
Cl1-Cl2	3.34(5)	N-N	6.48(2)
Cl1-Cl2	6.115(7)	N-N	6.48(2)
Cl1-Cl2	5.863(7)	N-C2	1.53(2)
Cl1-S	5.052(7)	N-C3	1.48(2)
Cl1-S	4.680(6)	N-C4	1.50(2)
Cl1-P	4.562(4)	C1-C2	1.54(2)
Cl1-N	3.257(13)	C5-C6	1.56(2)
Cl1-N	5.036(14)	C6-C7	1.50(3)
Cl1-N	4.806(12)	C9-C10	1.37(2)
Cl2-Cl2	6.482(7)	C9-C14	1.41(2)
Cl2-Cl2	6.482(7)	C10-C11	1.38(2)
Cl2-S	5.948(7)	C11-C12	1.41(3)
Cl2-P	3.152(6)	C12-C13	1.34(3)
Cl2-P	4.646(6)	C13-C14	1.40(3)
Cl2-N	4.407(14)	C15-C16	1.44(2)
Cl2-N	4.800(14)	C15-C20	1.40(2)
Cl2-N	4.608(12)	C16-C17	1.38(3)
		C17-C18	1.41(2)
		C18-C19	1.39(3)
		C19-C20	1.41(3)

<sup>a</sup> Numbers in parentheses are estimated standard deviations in the least significant digits.

## Acknowledgements

This manuscript was prepared while R.M.K. was Michael Guest Professor at the Weizmann Institute. This research was supported in part by a Ph.D. fellowship for B.K.V. from the Dutch Science Foundation (NWO) administered by the office for Chemical Research (SON) and a postdoctoral fellowship from the Royal Society to G.C..

The optical resolutions were carried out at Dutch State Mines (DSM), Geleen, Holland by W.H.J. Boesten. The cooperation of Prof. E.M. Meijer (DSM) and Dr. H.E. Schoemaker (DSM) is greatly appreciated.

## References

- 1 B.K. Vriesema, M. Lemaire, J. Buter, R.M. Kellogg, *J. Org. Chem.*, 51 (1986) 5169.
- 2 Some of the work described herein has appeared as preliminary communications: (a) B.K. Vriesema, R.M. Kellogg, *Tetrahedron Lett.*, 27 (1986) 1986; (b) G.A. Cross, R.M. Kellogg, *J. Chem. Soc., Chem. Commun.*, (1987) 1746.
- 3 (a) G. Consiglio, C. Botteghi, *Helv. Chim. Acta*, 56 (1973) 460; (b) G. Consiglio, F. Morandini, O. Picolo, *Tetrahedron*, 39 (1983) 2699; (c) G. Consiglio, T. Morandini, O. Picolo, *J. Chem. Soc., Chem. Commun.*, (1983) 112.
- 4 (a) T. Hayashi, M. Konishi, M. Fukushima, T. Mise, M. Kagobani, M. Tajika, M. Kumada, *J. Am. Chem. Soc.*, 104 (1982) 180; (b) see also P.W. Jolly, G. Wilke, *The Organic Chemistry of Nickel*, Academic Press, New York, 1975, Vol. II, p. 246–295; (c) J.P. Collman, L.S. Hegedus, *Principles and Applications of Organotransition Metal Chemistry*, University Science Books, Mill Valley, CA, 1980.
- 5 T. Hayashi, M. Konishi, M. Fukushima, K. Kanehira, T. Hioki, M. Kumada, *J. Org. Chem.*, 48 (1983) 2195.
- 6 J.H. Griffin, R.M. Kellogg, *J. Org. Chem.*, 50 (1985) 3261.
- 7 There is on the average about an 18% difference in the e.e.'s reported for the same ligands in refs. 5 and 6. Comparisons are therefore made between results obtained within one group rather than any cross comparisons. The reason for the difference in e.e.'s (no difference is observed in the absolute configurations of **3** obtained with various ligands) may lie in the fact that the rotation of neat **3** is very temperature dependent. We have used a value [5,6] of  $[\alpha]_D -5.91^\circ$  (neat) for optically pure (*R*-**3**). The observed rotation of neat **3** increases linearly  $0.18^\circ/^\circ\text{C}$  in the temperature range 16 to  $29^\circ\text{C}$ . For the data reported here the rotation of **3** obtained pure by GLC was measured in a 1 cm polarimeter cell kept at  $22.0 \pm 0.05^\circ\text{C}$  in a thermostatted polarimeter.
- 8 (a) A. Komiya, Y. Abe, A. Yamamoto, T. Yamamoto, *Organometallics*, 2 (1983) 1466; (b) T.T. Tsou, J.K. Kochi, *J. Am. Chem. Soc.*, 101 (1979) 6319, 7547.
- 9 K. Tatsumi, A. Nakamura, S. Komiya, A. Yamamoto, T. Yamamoto, *J. Am. Chem. Soc.*, 106 (1984) 8181.
- 10 For a theoretical analysis, see: J.S. Low, W.A. Goddard, III, *J. Am. Chem. Soc.*, 108 (1986) 6115.
- 11 This picture differs fundamentally from the dissociative mechanism found for some *trans*-square planar complexes: (a) K. Tatsumi, R. Hoffman, A. Yamamoto, J.K. Stille, *Bull. Chem. Soc. Jpn.*, 54 (1981) 1857; (b) F. Ozawa, T. Ito, Y. Nakamura, A. Yamamoto, *ibid.*, 54 (1981) 1868.
- 12 Grignard reagents are known to complex very readily with oxygen and amino groups, but we have found little information on complexation with sulfide and sulfoxide groups. For a recent review, see: W.E. Lindsell, in G. Wilkinson, F.G.A. Stone, E.W. Abel (Eds.), *Comprehensive Organometallic* Pergamon Press, Oxford, 1982, p. 156–205.
- 13 T.F. Lavine, *J. Biol. Chem.*, 169 (1947) 477.
- 14 B.W. Christensen, A. Kjaer, *J. Chem. Soc., Chem. Commun.*, (1965) 225.
- 15 R.E. Bowman, H.H. Stroud, *J. Chem. Soc.*, (1950) 1342.
- 16 J.A. Moore, D.E. Reed, *Org. Synth.*, Vol. V., 351.
- 17 S. Banfi, M. Cinquini, S. Colonna, *Bull. Chem. Soc. Jpn.*, 54 (1981) 1841.
- 18 (a) A.R. Katritzky, Y.K. Yang, *J. Chem. Soc., Perkin Trans. II*, (1984) 885; (b) A.R. Katritzky, C.M. Marson, *Angew. Chem. Int. Ed. Engl.*, 23 (1984) 420.
- 19 A. Kjaer, S. Wagner, *Acta Chem. Scand.*, 9 (1955) 721.
- 20 H. Hellman, F. Lingens, *Hoppe-Seyler's Zeit. Physiol. Chem.*, 297 (1954) 283.
- 21 W.H. ten Hoeve, H. Wynberg, *J. Org. Chem.*, 50 (1985) 4508.
- 22 (a) B.K. Vriesema, W.H. ten Hoeve, H. Wynberg, R.M. Kellogg, W.H.J. Boesten, E.M. Meijer, H.E. Schoemaker, *Tetrahedron Lett.*, (1986) 2045; see also (b) E.M. Meijer, W.H.J. Boesten, H.E. Schoemaker, J.A.M. van Balken, in J. Tramper, H.C. van der Plas, P. Linko (Eds.), *Biocatalysts in Organic Syntheses*, Elsevier Publishers, Amsterdam, 1985, p. 135–156.
- 23 See, for example: (a) B. Capon, S.A. McManus, *Neighboring Group Participation*, Plenum Press, New York, 1976, Vol. 1; (b) L. Birkofer, L. Morgenroth, *Chem. Ber.*, 96 (1963) 1909; (c) E.L. Eliel, D.E. Knox, *J. Am. Chem. Soc.*, 107 (1985) 2946.
- 24 This procedure was followed by T. Hayashi, M. Konishi, Y. Kobori, M. Kumada, T. Higuchi, K. Hirotsu, *J. Am. Chem. Soc.*, 106 (1984) 158 who investigated the coupling of primary alkyl Grignard and zinc reagents with aryl and vinyl halides catalyzed by  $\text{Pd}^0$  or  $\text{Ni}^0$  complexes.
- 25 E. Negishi, A. King, N. Okukado, *J. Org. Chem.*, 42 (1977) 1821.



- 26 D.G. Kaiser, G.J. Vangiessen, R.J. Reischer, W.J. Wechter, *J. Pharm. Sci.*, 65 (1976) 269.
- 27 A.L. Lehninger, *Biochemistry*, 2nd edit., Worth Publishers, Inc., New York, 1975, p. 208, 486, 489.
- 28 (a) G.H. Posner, J.P. Mallamo, M. Hulce, L.L. Frye, *J. Am. Chem. Soc.*, 104 (1982) 4180; (b) G.H. Posner, *Acc.Chem. Res.*, 20 (1987) 72.
- 29 R.E. Bowman, H.H. Stroud, *J. Chem. Soc.*, (1950) 1342.
- 30 M. Kitamoto, K. Kameo, S. Terashima, S.I. Yamada, *Chem. Pharm. Bull.*, 25 (1977) 1273.
- 31 H. Hellman, F. Lingens, *Hoppe-Seyler's Z. Physiol. Chem.*, 297 (1954) 283.
- 32 G. Germain, P. Main, M.M. Woolfson, *Acta Cryst. A*, 27 (1971) 360; updated 1982.